JOURNAL OF SOLID STATE CHEMISTRY 2, 61–67 (1970)

Magnetic Properties and Electronic Structure of Yttrium Hydrides

C. DEAN PARKS* AND WILLIAM G. BOS

Department of Chemistry, University of Louisville,
Louisville, Kentucky 40208

Received October 30, 1969

Magnetic susceptibilities are reported for yttrium metal and its hydrides in the temperature range 123–300°K. The theory of the paramagnetism of conduction band electrons and crystal field considerations are applied in the interpretation of the susceptibilities and yttrium Knight shifts and spin-lattice relaxation times of yttrium metal and its hydrides. Predictions regarding the nature and occupancy of the conduction band in the hydrides are made for the cases of protonic and hydridic hydrogen.

Introduction

Scandium (*1*), yttrium (*2, 3, 4*), and the lanthanide elements (*5*) form dihydrides that resemble the metallic hydrides (*6, 7, 8*) of several other transition elements. In metallic hydrides, a lower valence of the metal is used, electrical conductivity is of the same order of magnitude as that of the metal, and the conduction band electrons play a role in determining the magnetic properties. At pressures up to several atmospheres, scandium does not absorb hydrogen beyond the dihydride stage. Yttrium and most of the lanthanides form higher hydrides which approach the limiting composition, MH_3, at pressures less than one atmosphere. The trihydrides are similar to the saline hydrides of Groups Ia and IIa in that the stoichiometry corresponds to that predicted by the maximum positive valence of the metal, the electrical conductivity is greatly reduced from that of the metal and there appear to be no contributions from conduction band electrons to the magnetic properties.

The pressure–temperature–composition behavior of the yttrium–hydrogen system (*2, 3*) is similar to that of several of the heavy lanthanide–hydrogen systems. Up to about 0.2 hydrogen atoms per yttrium atom dissolve in the metal without a phase change. As additional hydrogen enters the metal, a hydrogen deficient dihydride phase begins to separate out. This hydride phase is face-centered cubic with respect to the metal atoms; the hydrogen occupies the tetrahedral interstices to give a fluorite structure (*4*). Between 1.9 and 2.2 H/Y this fluorite structure persists with the octahedral interstices beginning to fill. The further addition of hydrogen leads to the separation of a hydrogen deficient trihydride phase, hexagonal close-packed with respect to metal atoms, and between 2.2 and 2.7 H/Y the lower hydride is progressively converted to the higher. Above 2.7 H/Y, the addition of hydrogen is accompanied by rapidly increasing dissociation pressure. Lattice constants (*4*) are as follows: yttrium dihydride, $a_0 = 5.205$ Å, and yttrium trihydride, $a_0 = 3.674$ Å and $c_0 = 3.674$ Å.

The hydrogen in metallic hydrides has been described as being protonic, atomic, or hydridic in nature. General arguments for and against each of these viewpoints have been summarized by several authors (*6–8*). For scandium, yttrium and the lanthanide hydrides, the hydrogen nuclear magnetic resonance signal is unshifted from its position in diamagnetic compounds (*9*). This suggests that there is no unpaired electron density on the hydrogen species in these compounds and that the protonic or hydridic, but not the atomic, model applies.

The magnetic properties of metallic hydrides are of particular interest because they are closely related to the electronic structure of these compounds. For most of the lanthanide elements, the magnetic properties of the metals and the hydrides are dominated by unpaired *f* electrons in the atom cores (*5*). The conduction electrons provide a means by which coupling between the magnetic atom cores can occur. Magnetic ordering occurs at

---

* Present address: Department of Chemistry, Mississippi College, Clinton, Miss. 39056.

much lower temperatures in the hydrides than the corresponding metals. This reduced tendency toward ordering indicates decreased availability of the conduction electrons for coupling. Scandium, yttrium, and lanthanum have no *f* electrons. The relatively weak paramagnetism of the conduction band electrons can be detected and provides more direct information concerning the conduction band.

Schreiber and Cotts (*10*) have reported an extensive nuclear magnetic resonance study of lanthanum and its hydrides. Later, Schreiber (*9*) analyzed the Knight shifts and spin-lattice relaxation times for the metal nuclei in scandium, yttrium, and lanthanum metals and their dihydrides. After distinguishing *s*-spin, *d*-spin, and *d*-orbital contributions to the bulk susceptibilities, the Knight shifts and spin-lattice relaxation, Schreiber suggested that the hydrogen in these hydrides was protonic in nature. As has recently been pointed out, however, the available data can also be interpreted in terms of a hydridic model (*11*). The present work continues the discussion of the ambiguity in the interpretation of the magnetic properties and presents a more detailed analysis of the properties of yttrium metal and yttrium hydrides.

Experimental

The yttrium metal used in these experiments was obtained as ingots from the United Mineral and Chemical Corporation and was of purity designation 99.9%. A typical analysis provided by the manufacturer showed the following spectroscopically detectable impurities in ppm: Ca, 500; Dy, 100; Sm, 100; Er, 100; Gd, 50; Yb, 10; and Si and Mg, less than 100. Samples of 0.5-g weight were cut from the ingot using a tungsten carbide blade. They were polished under mineral oil with silicon carbide paper, then washed with acetone and ether. Samples to be used for the preparation of hydrides were placed in a molybdenum pan hanging by a quartz fiber from the beam of a Cahn Gram Electrobalance. Most of the weight of each sample was tared out so that a more sensitive scale could be used. The balance was enclosed in a vacuum chamber attached to a vacuum system and could be evacuated to less than 10^{-5}-Torr pressure. As soon as the metal sample was in place, a Pyrex hangdown tube was brought into place around the sample and joined to the vacuum chamber by a standard taper joint. The system was then evacuated and the sample was annealed at 525°C for one hour. Following this, pure hydrogen from an Elhygen electrolytic generator was introduced in the system up to a pressure of 50 cm. Absorption of hydrogen to form the dihydride was rapid at this temperature. Additional hydrogen was taken up by the sample as it was cooled to room temperature, and compositions up to $YH_{2.8}$ could be obtained in this way. Each sample was alternately heated to over 500°C and cooled to room temperature several times to insure reaction by all parts of the sample. Samples of the dihydride were obtained by evacuating the system at the higher temperature and then cooling. Samples of higher hydrogen content, up to $YH_{2.8}$, were obtained by evacuating the system after cooling to room temperature. At room temperature, samples did not lose hydrogen even under vacuum. In either case, the sample of the desired composition was dumped from the pan while the system was still evacuated. It passed through a Whitey 43S4 valve, attached to the end of the sample hangdown tube by a Swagelock connector, into a Pyrex sample tube. The valve and sample tube were transferred to an inert atmosphere box where the samples were ground to fine powders and sealed into sample tubes. The compositions reported for the hydride samples prepared in this way are estimated to accurate to less than 0.02-atom ratio units. X-ray diffraction powder patterns confirmed that all of the hydride samples used for susceptibility measurements contained the single phase expected for the composition of the sample.

The susceptibilities of yttrium metal, dihydride and trihydride were measured over the temperature range from 123–300°K by the Faraday method. Samples weighing approximately 10 mg were used for these determinations. Values of $H(dH/dx)$ of approximately 6×10^6 Oe^2 cm^{-1}, as measured using a platinum metal standard, were used. With most of the sample weight tared out, the Cahn electrobalance, operated in vacuum, was used to measure weight changes to an accuracy of ± 0.005 mg. Measurements were made below room temperature using liquid nitrogen, acetone Dry Ice and ice water coolants contained in an unsilvered Dewar flask surrounding the sample hangdown tube.

Results

The magnetic susceptibilities of Y metal, $YH_{2.10}$ and $YH_{2.81}$ are shown as a function of temperature in Fig. 1. Uncertainties in the points shown are less than $\pm 10 \times 10^{-6}$ emu/g atom, based on the standard deviations calculated from up to five measurements on each sample at each temperature. The estimated effect of impurities, assumed to behave as unquenched positive ions, is shown at the bottom of Fig. 1. For each material the data support an approximately linear temperature dependence over the range covered by the present study, 123–300°K.

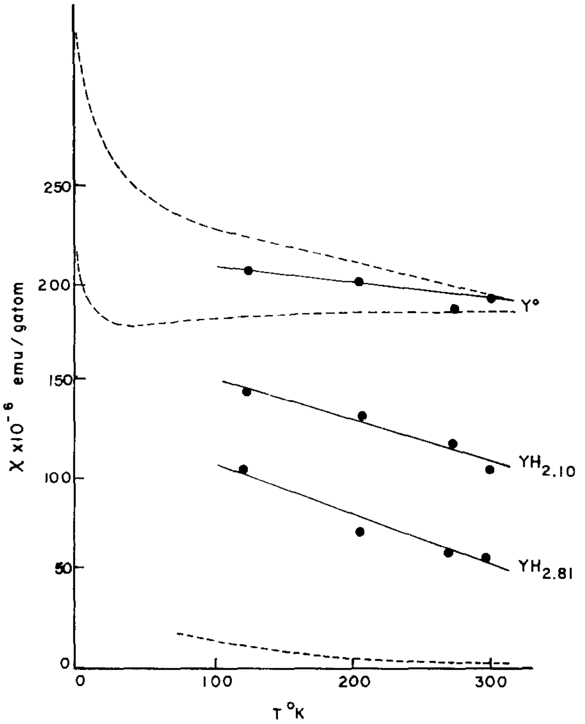

FIG. 1. Magnetic susceptibilities of yttrium metal and yttrium hydrides as a function of temperature. Other recent reports of the susceptibility of yttrium metal by Schumacher and Wallace (*13*) and by Gardner and Penfold (*12*) are shown by the dashed curves above and below the solid curve for the metal, respectively. The dashed curve at the bottom of the figure represents the estimated effect of impurities.

A significant portion of this temperature dependence of the measured susceptibility is probably due to the effect of impurities.

For Y metal, the recent reports by Gardner and Penfold (*12*) and by Schumacher and Wallace (*13*) are also shown in Fig. 1. The data of Gardner and Penford represent the most thorough study of the temperature dependence of the susceptibility available for Y metal. From approximately 50°K to room temperature, they observed a gradual decrease in the susceptibility with decreasing temperature. If corrected for impurities, the results of the present study agree with those of Gardner and Penfold within experimental error. Schumacher and Wallace (*13*) state that the temperature dependence, which they observed, can be accounted for by the effect of impurities.

For both of the yttrium hydrides, the susceptibility increases with decreasing temperature, but the rate of increase is slow compared to that predicted by a Curie law. The slightly greater temperature dependence of the hydrides' susceptibilities may be due to the destruction of the mechanism responsible for the positive temperature coefficient observed for the metal by Gardner and Penfold.

At room temperature, the susceptibility of $YH_{2.10}$ is just over one-half that of yttrium metal. A further decrease in the susceptibility occurs with the formation of the hydrogen deficient trihydride, $YH_{2.81}$. Compositions approaching the limiting composition YH_3 more closely cannot be achieved with hydrogen pressures of one atmosphere or less (*3*). The hydride of this limiting composition is expected to be diamagnetic. In the closely related lanthanum–hydrogen system, the change from paramagnetic to diamagnetic behaviour occurs at the composition $LaH_{2.7}$, and the susceptibility then becomes more negative with increasing hydrogen content (*14*). Lanthanum metal exhibits temperature dependent paramagnetism; however, the temperature dependence of the susceptibility disappears upon hydride formation (*13*).

Discussion

The magnetic susceptibilities and the related yttrium Knight shifts and nuclear spin-lattice relaxation times for the metal and for the dihydride are given in Table I. The yttrium metal Knight shift is taken from the data of Barnes et al. (*15*), the Knight shift for the dihydride from Schreiber's data (*9*) and the relaxation times from the report of Narath and Fromhold (*16*). For the dihydride, χ is reduced to about 0.55 of the value for the metal, K is about 1/3 of the value for the metal and $1/T_1T$ is nearly two orders of magnitude smaller than that of the metal. The different ways in which χ, K, and $1/T_1T$ are affected by hydride formation provide additional information concerning the electronic structure of the metal and the hydrides.

TABLE I

THE MAGNETIC PROPERTIES OF YTTRIUM METAL AND YTTRIUM DIHYDRIDE

	Y	YH_2
χ (emu g atom^{-1})	184×10^{-6}	104×10^{-6}
K (%)	0.34[a]	0.11[b]
$1/T_1T$ (sec^{-1} deg^{-1})	0.067[c]	0.0018[c]

[a] Ref. *15*.
[b] Ref. *9*.
[c] Ref. *16*.

The Magnetic Properties and Electronic Structure of Yttrium Metal

We begin our analysis of the magnetic properties by examining the data for yttrium metal. Following the procedure which has previously been applied to lanthanum and its hydrides (*11*) and to a variety of transition metals (*17–20*), we assume distinct *s*-spin, *d*-spin and *d*-orbital contributions to χ, K, and $1/T_1T$. While there is some question as to whether the electrons in the band can be distinguished as being *s* or *d*, this formulation provides a convenient method for recognizing the contributions of the atomic orbitals to the conduction band. Gschneidner (*21*) has recently provided a good explanation of the Hall coefficients for yttrium and several lanthanide metals on the basis of the numbers of *d* electrons and *s* holes in the band. In general, two factors may be distinguished as contributing to deviations from free electron behavior in the vicinity of the Fermi energy: (1) The *d* bands are relatively narrow and may contribute a high density of states, and (2) electron–phonon interactions enhance the contributions of a given density of states to such physical properties as specific heat and magnetic susceptibility (*22*). A rigorous treatment of either of these effects would require extensive knowledge of a variety of electronic and structural parameters. We take the effect of a high density of *d* states at the Fermi energy to be the more important and treat it explicitly. The density of states values used in the calculations below are those derived from specific heat measurements. Since the heat capacity and spin susceptibility deviate from the free electron predictions in a parallel manner (*23*), some compensation for electron–phonon interactions is implicit in our treatment.

On a per atom basis we write

$$\chi = \chi_s + \chi_d + \chi_0, \tag{1}$$

$$K = K_s + K_d + K_0, \tag{2}$$

$$\frac{1}{T_1T} = \frac{1}{T_{1s}T} + \frac{1}{T_{1d}T} + \frac{1}{T_{10}T}. \tag{3}$$

The individual contributions to χ, K, and $1/T_1T$ may be estimated using the set of equations which have been discussed in some detail earlier (*11*):

$$\chi_s = 2\beta^2 N_s(E_F). \tag{4}$$

$$K_s = 8\pi/3\langle|\psi_s(0)|^2\rangle_{E_F}\chi_s. \tag{5}$$

$$\frac{1}{T_{1s}T} = \frac{4\pi k}{\hbar}\left[\beta\gamma_n\hbar\frac{8\pi}{3}\langle|\psi_s(0)|^2\rangle_{E_F}\right]^2 N_s^2(E_F). \tag{6}$$

$$1/T_{1s}T = (4\pi k/\hbar)(\gamma_n^2/\gamma_e^2)K_s^2. \tag{7}$$

$$\chi_d = 2\beta^2 N_d(E_F). \tag{8}$$

$$K_d = 8\pi/3\langle\rho(0)\rangle\chi_d. \tag{9}$$

$$\frac{1}{T_{1d}T} = \frac{4\pi k}{\hbar}\left[\beta\gamma_n\hbar\frac{8\pi}{3}\langle\rho(0)\rangle\right]^2 N_d^2(E_F)q. \tag{10}$$

$$1/T_{1d}T = (4\pi k/\hbar)(\gamma_n^2/\gamma_e^2)K_d^2 q. \tag{11}$$

$$\chi_0 = (2\beta^2/5\Delta)n(n' - n) \tag{12}$$

$$K_0 = 2\langle r^{-3}\rangle D\chi_0. \tag{13}$$

$$\frac{1}{T_{10}T} = \frac{4k}{\hbar}[2\beta\gamma_n\hbar\langle r^{-3}\rangle d]^2 N_d^2(E_F)p. \tag{14}$$

Most of the symbols used here have their conventional meaning. $N_s(E_F)$ and $N_d(E_F)$ are the densities, for one direction of spin, of *s* states and *d* states, respectively, at the Fermi energy. $\langle|\psi_s(0)|^2\rangle_{E_F}$ is the density of *s* states at the nucleus and having energy near E_F. $\langle\rho(0)\rangle$ is the average *s*-spin density at the nucleus due to core polarization by *d*-electron spins. The factors q and p are defined as

$$q = \tfrac{1}{3}f + \tfrac{1}{2}(1 - f)^2 \tag{15}$$

and

$$p = \tfrac{2}{3}f(2 - \tfrac{5}{3}f), \tag{16}$$

where f is the relative weight of T_{2g} orbitals at E_F. Both q and p are less than unity and reflect the reduced efficiency with which *d* electrons contribute to nuclear spin-lattice relaxation. With r being the electron–nucleus distance, the averages $\langle r^{-3}\rangle_D$ and $\langle r^{-3}\rangle_d$ are for all of the *d* electrons in the conduction band and for the *d* electrons at E_F, respectively; n is the number of *d* electrons in the band and n' the capacity of the *d* band per metal atom.

To the extent that the terms in Eqs. (4)–(14) are known or can be estimated, the individual contributions to χ, K, and $1/T_1T$ can be evaluated. The number of contributions which must be calculated independently is reduced through the use of Eqs. (1)–(3) which relate the individual contributions to the measured values of each property. A further reduction in the number of independent calculations is possible through the use of Eqs. (7) and (11) which relate K_s and $1/T_{1s}T$ and K_d and $1/T_{1d}T$, respectively.

The density of states at E_F,

$$N(E_F) = N_s(E_F) + N_d(E_F), \tag{17}$$

is obtained as 2.1 states eV^{-1} atom^{-1} from specific heat measurements on yttrium metal (*24*). Combining Eqs. (4) and (8) and using this value, we obtain

$$\chi_{\text{spin}} = \chi_s + \chi_d = 2.30 \times 10^{-28}\ \text{emu atom}^{-1}. \tag{18}$$

In the free electron approximation (*25*), the diamagnetism of the conduction band electron is

$$\chi_{\text{dia}} = \tfrac{1}{3}\chi_{\text{spin}} = 7.66 \times 10^{-29}\ \text{emu atom}^{-1} \tag{19}$$

The total paramagnetic susceptibility, obtained by correcting the measured susceptibility for the diamagnetism of both the Y^{3+} core electrons and the conduction electrons, is 3.67×10^{-28} emu atom^{-1}. With these results and Eq. (1), we obtain

$$\chi_0 = \chi_{\text{para}} - \chi_{\text{spin}} = 1.76 \times 10^{-28} \text{ emu atom}^{-1}. \qquad (20)$$

Next we obtain an estimate of K_0 using Eq. (13) and a value of $\langle r^{-3}\rangle_D$ obtained from the hyperfine splitting of the ground term of the free Y atom. The hyperfine splitting, δ, is 530.4 cm^{-1} (*30*). We relate δ to $\langle r^{-3}\rangle_D$ as follows (*27*):

$$\delta = 2.91\ HZ(2l+1)\langle r^{-3}\rangle. \qquad (21)$$

Here, $H = 1.00$ is a relativistic correction factor, $Z = 24.5$ is the effective nuclear charge (*28*) and $l = 2$ for the $4d$ electron in the yttrium atom. For yttrium metal we take $\langle r^{-3}\rangle_D$ as $\frac{3}{4}$ of the free-electron value because the electron is delocalized in the conduction band (*17*). Upon substitution, Eq. (13) yields

$$K_0 = 2\langle r^{-3}\rangle_D \chi_0 = 0.26\,\%. \qquad (22)$$

From this and the measured K, we obtain, using Eq. (2):

$$K_s + K_d = K - K_0 = 0.08\,\%. \qquad (23)$$

In order to treat the yttrium nuclear spin-lattice relaxation times, an assumption relating to the values of q and p is necessary. We will assume that the E_g and T_{2g} are mixed uniformly throughout the d band. Then, at E_F, $f = 3/5$ and we obtain $q = 0.2$ and $p = 0.4$. An alternate choice of q and p will be considered shortly. Although $\langle r^{-3}\rangle$ may be different for the d electrons at E_F than for all of the d electrons, we take $\langle r^{-3}\rangle_d = \langle r^{-3}\rangle_D$ as an approximation. Also, to a good approximation, we take $N_d(E_F) = N(E_F)$. The schematic band structure shown for yttrium metal in Fig. 2 is similar to that proposed by Gschneidner (*29*) to account for the Hall coefficient of yttrium and several lanthanide metals. The ns band and $(n-1)$ d bands overlap with E_F near the top of the s band. Both the relatively flat shape of the s band and position of E_F favor a very low density of s states at E_F. Using these assumptions, Eq. (14) yields

$$\frac{1}{T_{10}T} = 0.044 \text{ sec}^{-1} \text{ deg}^{-1}. \qquad (24)$$

This result together with Eq. (3) yields

$$\frac{1}{T_{1s}T} + \frac{1}{T_{1d}T} = \frac{1}{T_1 T} - \frac{1}{T_{10}T} = 0.023 \text{ sec}^{-1} \text{ deg}^{-1}. \qquad (25)$$

Equations (7), (11), (23), and (25) represent four equations in the four unknowns K_s, K_d, $1/T_{1s}T$ and $1/T_{1d}T$. The results of the simultaneous solution of these equations are given in Table II along with a summary of all of the contributions estimated above. The s-spin and d-spin contributions to χ have not been separated. As has been pointed out above, the density of s states at E_F is probably very small. It is likely, therefore, that χ_s is small and χ_{spin} is dominated by χ_d.

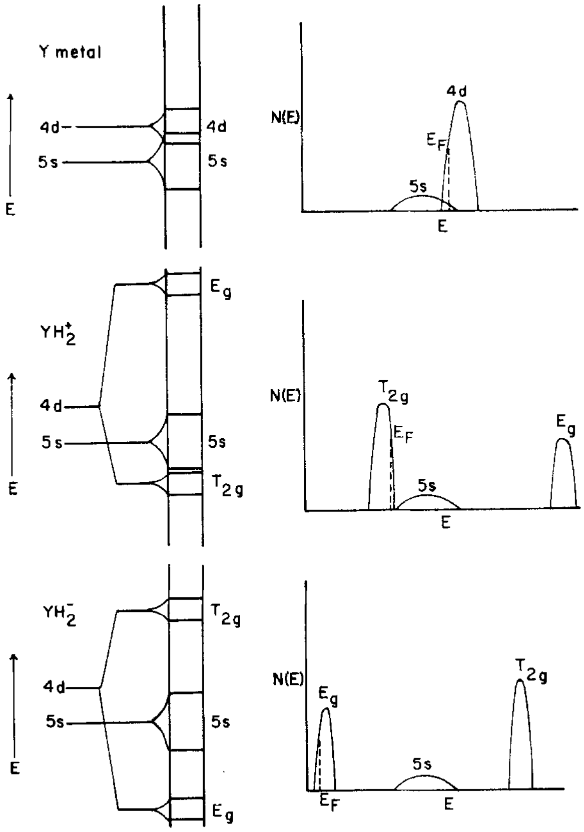

FIG. 2. Schematic diagrams of the crystal field splitting patterns and conduction band densities of states for yttrium metal and for yttrium dihydrides assuming the protonic or hydridic model.

The results of this analysis are not very sensitive to the choice of values of p and q. Yttrium metal is hexagonal close-packed. In the case of the closely related face-centred cubic structure, crystal field effects act to lower the energy of the T_{2g} orbitals relative to the E_g orbitals (*29*). If it is assumed that in yttrium metal the T_{2g} levels are lowered relative to the E_g levels to the extent that only the T_{2g} levels occur at the Fermi energy, then $q = \frac{1}{3}$ and $p = \frac{2}{9}$. The effects of this alternate assumption on the analysis of the magnetic properties are shown in the lower half of Table II. The estimates of contributions to χ are unaffected by the choice of p and q. Although only the contributions to relaxation depend explicitly on p and q, the method used to estimate the contributions

TABLE II

SPIN AND ORBITAL CONTRIBUTIONS TO THE SUSCEPTIBILITY, KNIGHT SHIFT AND SPIN-LATTICE RELAXATION IN YTTRIUM METAL

	Experimental	Total Paramagnetism	*s* spin	*d* spin	*d* orbital
Case 1: $p = 4/10, q = 2/10$					
$\chi_{\text{para}} \times 10^{28}$ emu atom^{-1}	3.29	4.05	(2.30)		1.75
K_y %	0.34[a]	—	0.28	−0.20	0.26
$\frac{1}{T_1T}$ sec^{-1} deg^{-1}	0.066[a]	—	0.022	0.001	0.043
Case 2: $p = 2/9, q = 1/3$					
$\chi_{\text{para}} \times 10^{28}$ emu atom^{-1}	3.29	4.05	(2.30)		1.75
K_y %	0.34[a]	—	0.20	−0.13	0.27
$\frac{1}{T_1T}$ sec^{-1} deg^{-1}	0.066[a]	—	0.037	0.005	0.024

[a] Ref. *16*.

to K introduce slight differences in these quantities. The major effect of alternate choices of p and q is in the estimates of contributions to relaxation. Though $N_s(E_F)$ and, therefore, χ_s are probably small, the *s* contributions to the nuclear magnetic resonance properties are significant regardless of the choice of p and q. This is consistent with the general finding that, per spin, the field resulting from *s* electrons is an order of magnitude larger than that for *d* electrons (*30*). The *d*-spin and *d*-orbital contributions to $1/T_1T$ are further reduced by the factors q and p, respectively.

The Magnetic Properties and Electronic Structure of Yttrium Hydrides

In treating the reduced values of χ, K, and $1/T_1T$ in yttrium dihydride, it is important to recognize that the individual contributions to each of these properties may be reduced from those in the metal by either of two mechanisms. Whether electrons are added to the conduction band or removed from the conduction band, $N_s(E_F)$, $N_d(E_F)$ and $n(n' - n)$ may all decrease. Because of this, the fact that χ, K, and $1/T_1T$ decrease in YH_2 does not, in itself, provide a means for distinguishing between the protonic and hydridic models.

In order to account for the limiting composition of yttrium and lanthanide hydrides, MH_3, the protonic model requires that crystal field effects split the conduction band in such a way as to give a lower band with a capacity of six electrons per metal atom (*9*). The application of crystal field arguments to these hydrides has not been reported in detail. Merriam and Schreiber have, however, suggested one possible band scheme (*31*). They suggest that a lower lying *d* band, with a capacity of four electrons per metal atom, overlaps with the *s* band to give the required total capacity. From our examination of the problem, this proposed splitting pattern appears to be incorrect.

The arrangement of metal and hydrogen atoms in yttrium and most lanthanide dihydrides is that of the fluorite structure. Hydrogens occupy the tetrahedral interstices of the face-centered cubic array of metal atoms. Each metal atom is surrounded by eight hydrogen atoms located at the corners of a cube. The five *d* orbitals of the metal atom fall into two classes, E_g and T_{2g}, under the symmetry of this structure. The cubic arrangement of hydrogen atoms may be considered as two interpenetrating tetrahedra around the metal atom. The direction of splitting here is then the same as that for tetrahedral complexes and opposite to that of octahedral complexes.

Figure 2 gives band diagrams for the metal and for the dihydride assuming either protonic hydrogen or hydridic hydrogen. In the protonic model, the T_{2g} orbitals of the metal are lowered in energy relative to the E_g orbitals. The *s* band is placed above the T_{2g} band so that the capacity of the lowest band is limited to six electrons per metal atom. The absence of *s* character at E_F is consistent with the long spin-lattice relaxation time for yttrium in the dihydride. The electrons lost by the hydrogen in forming protons fill the T_{2g} band to five sixths of its capacity.

In the hydridic model, the assignment of a negative charge to the hydrogen species results in a lowering of the energy of the E_g orbitals relative to the T_{2g} orbitals. The *s* band is placed above E_F to account for the long yttrium spin-lattice relaxation time in the dihydride. One electron per metal atom occupies the conduction band in the dihydride.

The position of Fermi energy is shown for the dihydride in Fig. 2 for each of the models. The extension of either model to the trihydride is straightforward. According to the protonic model, the T_{2g} band would be filled in the trihydride. The hydridic model, on the other hand, attributes the limiting composition to the complete depopulation of the E_g band. Either point of view is consistent with the absence of metallic character in the trihydride.

The analysis of the magnetic properties does not provide a means for distinguishing between the protonic and hydridic models. It does, however, provide valuable information concerning the nature of the conduction band in the hydrides. According to the protonic model, the electron configuration of the metal is d^5 in the dihydride and d^6 in the trihydride. The hydridic model predicts an electron configuration for the metal of d^1 in the dihydride and d^0 in the trihydride. The isomer shift of Mössbauer spectral lines (*32*) is sensitive to just such changes in electronic structure. We have recently reported the isomer shifts of ^{161}Dy in dysprosium metal and several dysprosium compounds (*33*). The results which were obtained for dysprosium hydrides, which closely resemble yttrium hydrides, strongly supported the view that the hydrogen present in these compounds is hydridic in nature. Heckman (*34*) recently reported positive Hall coefficients for cerium hydrides and interpreted them in terms of a protonic model. Libowitz and Pack (*35*) have since used a hydridic model to explain both the positive Hall coefficients and the results of their own resistivity measurements for cerium hydride single crystals. Rather direct evidence supporting the hydridic model is provided by the decreasing intensity at the L_{III} X-ray emission edge in the series La metal $> LaH_{2.18} > LaH_{2.45} > LaH_{2.88}$ (*36*).

Acknowledgments

This work was supported by a grant from the National Science Foundation. C.D.P. held a Tennessee Eastman Graduate Fellowship in 1967–1968.

References

1. K. I. Hardcastle and J. C. Warf, *Inorg. Chem.* **5**, 1728 (1966).

2. C. E. Lundin and J. P. Blackledge, *J. Electrochem. Soc.* **109**, 838 (1962).

3. L. N. Yannopoulos, R. K. Edwards, and P. G. Wahlbeck, *J. Phys. Chem.* **69**, 2510 (1965).

4. A. Pebler and W. E. Wallace, *J. Phys. Chem.* **66**, 148 (1962).

5. W. G. Bos and K. H. Gayer, *J. Nucl. Mater.* **18**, 1 (1966).

6. G. G. Libowitz, "The Solid State Chemistry of Binary Metal Hydrides," W. A. Benjamin, Inc., New York, 1965.

7. T. R. P. Gibb, *in* "Progress in Inorganic Chemistry," (F. A. Cotton, Ed.), Vol. 3, p. 315, Interscience, New York, 1962.

8. Y. Ebisuzaki and M. O'Keeffe, *in* "Progress in Solid State Chemistry," (H. Reiss, Ed.), Vol. 4, p. 187, Pergamon Press, Oxford, 1967.

9. D. S. Schreiber, *Phys. Rev.* **137**, A860 (1965).

10. D. S. Schreiber and R. M. Cotts, *Phys. Rev.* **131**, 1118 (1963).

11. W. G. Bos and H. S. Gutowsky, *Inorg. Chem.* **6**, 552 (1967).

12. W. E. Gardner and J. Penfold, *Phys. Lett.* **26A**, 204 (1968).

13. D. P. Schumacher and W. E. Wallace, *Inorg. Chem.* **9**, 1563 (1966).

14. B. Stalinski, *Bull. Acad. Pol. Sci., Classe III* **5**, 997 (1957).

15. R. G. Barnes, F. Borsa, S. L. Segal, and D. R. Torgeson, *Phys. Rev.* **137**, A1828 (1965).

16. A. Narath and T. Fromhold, Jr., *Phys. Lett.* **25A**, 49 (1967).

17. J. Butterworth, *Proc. Phys. Soc.* **83**, 71 (1964).

18. Y. Yafet and V. Jaccarino, *Phys. Rev.* **133**, A1630 (1964).

19. A. M. Clogston, V. Jaccarino, and Y. Yafet, *Phys. Rev.* **134**, A650 (1964).

20. J. A. Seitchik, A. C. Gossard, and V. Jaccarino, *Phys. Rev.* **136**, A1119 (1964).

21. K. A. Gschneidner, *in* "Rare Earth Research III," (L. Eyring, Ed.), p. 153, Gordon and Breach, New York, 1965.

22. T. L. Loucks, *Phys. Rev.* **144**, 504 (1966).

23. C. Kittel, "Introduction to Solid State Physics," p. 293, John Wiley and Sons, New York, 1965.

24. F. J. Morin and J. P. Maita, *Phys. Rev.* **129**, 1115 (1963).

25. A. H. Wilson, "The Theory of Metals," 2nd ed., p. 164, Cambridge University Press, London, 1953.

26. National Bureau of Standards Circular 467, Vol. III, p. 196.

27. H. B. G. Casimir, "On the Interaction Between Atomic Nuclei and Electrons," 2nd ed., p. 34–55. W. H. Freeman and Company, San Francisco, 1963.

28. G. J. Ritter, *Phys. Rev.* **126**, 240 (1962).

29. J. Calloway, "Energy Band Theory," p. 193–4, Academic Press, New York, 1964.

30. R. E. Watson and A. J. Freeman, *Phys. Rev.* **123**, 198 (1963).

31. M. F. Merriam and D. S. Schreiber, *J. Phys. Chem. Solids* **24**, 1375 (1963).

32. D. A. Shirley, *Rev. Mod. Phys.* **36**, 339 (1964).

33. T. P. Abeles, W. G. Bos, and P. J. Ouseph, *J. Phys. Chem. Solids*, **30**, 2159 (1969).

34. R. C. Heckman, *J. Chem. Phys.* **40**, 2158 (1967).

35. G. G. Libowitz and J. G. Pack, *J. Chem. Phys.* **50**, 3557 (1969).

36. A. C. Sarma and W. G. Bos, to be published.